EUKARYOTIC CELL, Sept. 2007, p. 1606–1617 Vol. 6, No. 9
1535-9778/07/$08.00+0 doi:10.1128/EC.00260-07

A *Toxoplasma gondii* Leucine-Rich Repeat Protein Binds Phosphatase Type 1 Protein and Negatively Regulates Its Activity▽

Wassim Daher,[1]† Gabrielle Oria,[2] Sylvain Fauquenoy,[2] Katia Cailliau,[3] Edith Browaeys,[3] Stanislas Tomavo,[2]* and Jamal Khalife[1]*

Unité INSERM 547/IPL, Institut Pasteur, 1 rue du Prof. Calmette, B.P. 245, 59019 Lille Cedex, France[1]*; Equipe de Parasitologie Moléculaire, CNRS UMR 8576, Université des Sciences et Technologies de Lille, 59655 Villeneuve d'Ascq Cedex, France*[2]*; and UPRES EA 1033, IFR 118, SN3, Université des Sciences et Technologies de Lille, 59655 Villeneuve d'Ascq, France*[3]

Received 19 July 2007/Accepted 19 July 2007

We have characterized the *Toxoplasma gondii* protein phosphatase type 1 (TgPP1) and a potential regulatory binding protein belonging to the leucine-rich repeat protein family, designated TgLRR1. TgLRR1 is capable of binding to TgPP1 to inhibit its activity and to override a G_2/M cell cycle checkpoint in *Xenopus* oocytes. In the parasite, TgLRR1 mRNA and protein are both highly expressed in the rapidly replicating and virulent tachyzoites, while only low levels are detected in the slowly dividing and quiescent bradyzoites. TgPP1 mRNA and protein levels are equally abundant in tachyzoites and bradyzoites. Affinity pull down and immunoprecipitation experiments reveal that the TgLRR1-TgPP1 interaction takes place in the nuclear subcompartment of tachyzoites. These results are consistent with those of localization studies using both indirect immunofluorescence with specific polyclonal antibody and transient transfection of *T. gondii* vector expressing TgLRR1 and TgPP1. The inability to obtain stable transgenic tachyzoites suggested that overexpression of TgLRR1 and TgPP1 may impair the parasite's growth. Together with the activation of *Xenopus* oocyte meiosis reinitiation, these data indicate that TgLRR1 protein could play a role in the regulation of the *T. gondii* cell cycle through the modulation of phosphatase activity.

The protozoan *Toxoplasma gondii* is an obligate intracellular parasite that commonly infects humans and occasionally causes opportunistic disease. Recrudescence of a latent infection in immunodeficient individuals can result in encephalitis (30). Transplacental transmission of *T. gondii* can cause spontaneous abortion, mental retardation, and blindness (6). *T. gondii* is acquired primarily through the ingestion of sporulated oocysts containing sporozoites, which are shed by the definitive host (felids) or by ingestion of undercooked meat harboring bradyzoite tissue cysts. The cyst wall is digested during transit through the gastrointestinal tract, releasing the bradyzoites/sporozoites, which penetrate the intestinal epithelium where they immediately differentiate into rapidly dividing tachyzoites. Tachyzoites disseminate and proliferate during the acute stage of infection before differentiating into bradyzoites, which encyst in muscle tissue and the central nervous system, thereby establishing a chronic infection (2). Thus, the parasite has a complex life cycle involving asexual and sexual stages in the infected host. This cycle includes a rapidly growing tachyzoite and a slowly dividing bradyzoite form. The ability of this parasite to cycle between the two forms is fundamental for its survival and is also considered a key event involved in pathogenesis by *T. gondii* (18, 27). Several studies that implicated the switch between these two developmental stages revealed the expression of stage-specific genes whose products can account for the differences in replication rates and metabolism displayed by tachyzoites and bradyzoites (10, 22, 31, 34, 40). We assume that posttranslational regulation, such as phosphorylation/dephosphorylation, as largely described in other biological systems, can also be required for the modulation and progression of the parasite's life cycle. In this context, significant progress has been made in characterizing several *T. gondii* kinases (36). However, very little is known about protein phosphatases (PPs) and their regulators in the parasite. The dephosphorylation of phosphoproteins is in general catalyzed by tyrosine phosphatases and serine/threonine phosphatases. In *T. gondii*, a number of putative sequences and phosphatase activities have been reported, including molecular characterization of a phosphatase type 2C that controls the dynamics of actin (13, 24). More recently, proteomic studies confirmed the presence of peptide sequences with homology to protein phosphatase 2C in the rhoptries of *T. gondii* (5, 21), and the expression of protein phosphatase type 1 (PP1) activity in tachyzoites was reported (14). This activity was found to be insensitive to inhibitors of PP2A but sensitive to a specific PP1 inhibitor and was recognized by anti-PP1 antibodies, suggesting that PP1 activity is likely involved in some aspects of the *T. gondii* life cycle and development. In various organisms, PP1, which exhibits an extremely high degree of sequence conservation throughout evolution, regulates important cellular processes, including protein synthesis, glycogen metabolism, transcription, and cell cycle progression (3, 7). It is becoming

* Corresponding author. Mailing address for Jamal Khalife: Unité INSERM 547, Institut Pasteur de Lille, 1 rue du Prof. Calmette, 59019 Lille, France. Phone: 33320877968. Fax: 33320877888. E-mail: jamal.khalife@pasteur-lille.fr. Mailing address for Stanislas Tomavo: CNRS UMR 8576, Université des Sciences et Technologies de Lille, 59655 Villeneuve d'Ascq, France. Phone: 33320436941. Fax: 33320436555. E-mail: stan.tomavo@univ-lille1.fr.

† Present address: Department of Microbiology and Molecular Medicine, Centre Medical Universitaire, University of Geneva, 1 Rue Michel-Servet, 1211 Geneva, Switzerland.

▽ Published ahead of print on 27 July 2007.

increasingly clear that the diverse functions of PP1 are directed by interaction with regulatory subunits. In *Schizosaccharomyces pombe*, the expression of a PP1 regulator, $Sds22^+$, was shown to be essential for progression from metaphase to anaphase, by enhancing PP1 activity. Recent examination of the orthologous gene of $Sds22^+$ in *Plasmodium falciparum*, which we named *P. falciparum* leucine-rich repeat type 1 (PfLRR1), revealed that the gene product interacts with PfPP1. Functional studies with *Xenopus* oocytes revealed that PfLRR1 interacts with endogenous PP1 and overcomes the G_2/M cell cycle checkpoint by promoting progression to germinal vesicle breakdown (GVBD) (11). In contrast to the situation in yeast, the process of cell replication involving PfLRR1 was shown to be due to an inhibition of PP1 activity rather than to its enhancement.

Here we report the molecular and functional characterization of the *T. gondii* ortholog of PfLRR1, designated TgLRR1, and its target gene product, TgPP1. Our findings indicate for the first time that TgLRR1 interacts with TgPP1 in the nuclear compartment of the rapidly replicating tachyzoites and may inhibit its activity. Furthermore, we show that TgLRR1 can also trigger the progression of physiologically arrested *Xenopus* oocytes to meiosis. These data suggest that the inhibition of nuclear TgPP1 by TgLRR1 may contribute to cell cycle progression in *T. gondii*.

MATERIALS AND METHODS

Host cells and parasite cultures. The *T. gondii* 76K strain was serially passaged in human foreskin fibroblasts (HFF) grown in Dulbecco's modified Eagle's medium (DMEM; Biowhittaker, Belgium) supplemented with 10% fetal calf serum (FCS) (Dutscher), 2 mM glutamine (Sigma), and 0.05 mg · ml^{-1} gentamicin (Sigma). Tachyzoites were purified by membrane filtration as previously described (17). Encysted bradyzoites were purified from the brains of chronically infected mice as previously described (16).

Identification of *T. gondii* PP1 and TgLRR1 homolog genes. To identify the *T. gondii* PP1 gene, the *T. gondii* database (ToxoDB.org) was queried by TBLASTN, with the open reading frames (ORFs) of human and *P. falciparum* PP1 (accession numbers P62136 and AAM54063, respectively). Public database analyses allowed us to find three possible open reading frames in the ToxoDB database (TgGlmHMM_2112, TgTigrScan_5645, and TgGeneFinder_5784) which showed a high degree of identity with PP1. To obtain the correct and full-length cDNA, we performed three PCRs using three sets of primers covering the three complete putative ORFs predicted by ToxoDB. Primers used were 5′-ATGATCAACGAAGCATGGAAGGTCACTGTG-3′ and 5′-TTATTTGGCCATGCCTTTCTTCTTTTCCAC-3′ for TgGlmHMM_2112, 5′-ATGGAATTGCTGACTGAACGGCTGTATGCG-3′ and 5′-TTACGGATGTAGGCACTGCTACATCGTCGG-3′ for TgTigrScan_5645, and 5′-ATGGTGTCATTAGACGTCGATGTCGACGCC-3′ and 5′-TTATTTGGCCATGCCTTTCTTCTTTTCCAC-3′ for TgGeneFinder_5784. Only the third set of primers gave us a PCR product corresponding to the predicted size. The PCR product was then cloned in TOPO 2.1 TA cloning vector (Invitrogen) and sequenced using a dye terminator cycle sequencing kit and analyzed on an ABI Prism 377 DNA sequencer (Perkin-Elmer Biosystems).

To experimentally identify the correct gene prediction for TgTwinScan_3263 (TgLRR1), the following primers were synthesized: 5′-ATGCCGGACGACACGAGGACAGCAGGACCCCCAGC-3′ and 5′-TCAAGCGTTGTGCTTCATAATGGACTTCTGCTTTG-3′. These primers were employed in reverse transcriptase PCR (RT-PCR) as previously described (11). The PCR products were then cloned in TA cloning vector and sequenced. To confirm the start and stop codons, 5′ and 3′ rapid amplification of cDNA ends (RACE) procedures were carried out using a Smart kit (Biosciences Clontech). The 5′ and 3′ ends of TgLRR1 were obtained by using the reverse primer 5′-GGATTTCTCGAATTCTGTTGC-3′ and the forward primer 5′-CGCGACGCTCACGGAGCTCAAAG-3′, respectively, and the adaptor primer according to the manufacturer's instructions. For TgPP1, the forward primer 5′-ATGGTGTCATTAGACGTCGATGTCGACGCC-3′ and the reverse primer 5′-TTATTTGGCCATGCCTTTCTTCTTTTCCAC-3′ were used. Analysis of TgPP1 and TgLRR1 proteins was performed by DNA Star ClustalW software and the Pfam database (http://www.sanger.ac.uk) and the Conserved Domain Database (http://www.ncbi.nlm.nih.gov/Structure/cdd/wrpsb.cgi).

Recombinant protein expression and antiserum production. The entire TgLRR1 cDNA obtained by PCR with the primers cited above was inserted into pET32a using the BamHI and HindIII sites and was verified by sequencing. Expression was carried out in the *Escherichia coli* BL21 strain. For TgPP1, the same system was used to express the active recombinant protein. The primers spanning the complete cDNA with BamHI and NotI restriction sites for subcloning were 5′-ATGGTGTCATTAGACGTCGATGTCGACGCC-3′ and 5′-TTATTTGGCCATGCCTTTCTTCTTTTCCAC-3′. In all experiments, expression and purification steps were carried out according to the manufacturer's instructions. For the purification of TgPP1, denaturing conditions were required as the protein was found in the inclusion bodies. In the case of TgLRR1, the recombinant protein was purified under native conditions. The His_6-tagged proteins were purified using Ni^{2+} chelation chromatography. The imidazole-eluted proteins were dialyzed against phosphate-buffered saline (PBS) containing 10% glycerol. Purity, checked by sodium dodecyl sulfate-polyacrylamide gel electrophoresis (SDS-PAGE) followed by Coomassie blue staining, was >95%.

For antiserum production, the purified TgLRR1 was mixed with complete Freund's adjuvant (100 μg per injection) and subcutaneously injected into mice. Animals were boosted 4 weeks later with the same quantity in Freund's incomplete adjuvant. The serum was obtained 2 weeks after the last boost. Serum was tested for its titer and specificity by enzyme-linked immunosorbent assay and Western blotting against recombinant protein. The serum raised against TgLRR1 was preadsorbed on thioredoxin recombinant protein. Because of the high degree of homology among PP1 of all species, the antiserum raised against PfPP1 was used in this study.

Assays for PP1 activity. The activity of recombinant TgPP1 (rTgPP1) with *p*-nitrophenyl phosphate (pNPP) as substrate was assayed essentially as previously described (11, 12). The initial rate of liberation of *p*-nitrophenol was determined spectrophotometrically at 405 nm. To normalize the phosphatase activity of rTgPP1 obtained from different batches, a standard curve was constructed with rabbit recombinant PP1 (New England Biolabs), and 5 units of rTgPP1 was defined as the activity giving 1 absorbance unit over 1 h of reaction. The activity of rTgPP1 was assayed at 37°C in a reaction mixture volume of 200 μl containing 50 mM Tris (pH 7.5), 0.1 mM EDTA, 0.5 mM dithiothreitol, 1 mM $MnCl_2$, and 5 mM pNPP. In some experiments, the effect of okadaic acid, a well-known phosphatase inhibitor (29), was added at different concentrations in the PP1 assay. Results are the averages of triplicate assays of three batches of rTgPP1.

To study the effect of rTgLRR1 on rTgPP1 activity, the same procedure was used. Briefly, different amounts of rTgLRR1 were added to 5 units of rTgPP1 and preincubated for 1 h at room temperature before the rTgPP1 phosphatase activity was tested. As a negative control, the TgLRR1 was replaced with recombinant thioredoxin protein produced from the pET32a plasmid at the same concentrations. Results are the averages of three experiments.

Western blotting analysis. To detect and evaluate the protein levels of TgLRR1 and TgPP1, a total of 5×10^6 equivalent tachyzoites and 5×10^2 cysts (corresponding to bradyzoites) isolated from chronically infected mice were boiled in loading buffer (6.25 mM Tris-HCl [pH 6.8], 2% SDS, 10% sucrose) for 5 min, and one-fifth of the extract was separated by SDS-PAGE on a 12% polyacrylamide gel. After electrophoresis, proteins were transferred onto a nitrocellulose sheet by using a semidry transfer apparatus. The membranes were probed with anti-TgLRR1 or anti-PP1 antibodies at 1:100 dilution. To ensure that equal amounts of protein extracts from each parasitic stage were being loaded, a monoclonal antibody specific to actin was used at 1:1,000 dilution. A horseradish peroxidase-labeled anti-mouse immunoglobulin G (IgG) (1:1,000 dilution) was used as a secondary antibody, followed by chemiluminescence detection.

Subcellular protein extraction. The cytoplasmic and nuclear extracts were prepared according to a method previously described by Kibe et al. (26). Briefly, 10^9 purified tachyzoites were resuspended with 2 ml of lysis buffer A (10 mM HEPES [pH 7.9], 1.5 mM $MgCl_2$, 10 mM KCl, 0.5 mM dithiothreitol [DTT], 0.1 M EDTA, 0.65% NP-40, 0.5 mM phenylmethylsulfonyl fluoride [PMSF], and protease inhibitor cocktail [Roche]) and incubated for 10 min on ice. After centrifugation at 4,000 rpm for 10 min at 4°C, the supernatant corresponding to the cytoplasmic extract was harvested. To extract the nuclear proteins, the remaining pellet was resuspended in 200 μl of lysis buffer B (20 mM HEPES [pH 7.9], 1.5 mM $MgCl_2$, 420 mM NaCl, 0.5 mM DTT, 0.2 M EDTA, 25% glycerol, 0.2 mM PMSF, and protease inhibitor cocktail [Roche]) and incubated for 15 min on ice. The nuclear extract was cleared by centrifugation at 14,000 rpm for

10 min at 4°C. The supernatant corresponding to the nuclear extract was harvested and completed to a final volume of 2 ml with lysis buffer A. Both cytoplasmic and nuclear extracts were kept at −20°C until used in Western blotting experiments. To check the quality of extracts, the blots were probed with anti-lactate dehydrogenase type 1 (anti-LDH1), a cytoplasmic marker (1, 19), and anti-*T. gondii* DNA repair enzyme (anti-TgDRE), which is specific to a nuclear protein (15). For total protein extracts, 10^9 tachyzoites were incubated in 2 ml of lysis buffer A for 30 min at 4°C, followed by three consecutive freeze-thaw cycles with intermediate sonication steps. The supernatants were recovered and kept at −20°C until use.

Microcystin agarose affinity column and coimmunoprecipitation experiments. To isolate the TgLRR1-TgPP1 complex, microcystin beads, known to bind to PP1, were used. To this end, total protein extracts (corresponding to 1.75×10^9 parasites) prepared as described above, cytoplasmic or nuclear fractions (extracts from 10^9 parasites), were incubated overnight at 4°C with 100 μl of microcystin agarose beads (Upstate Biotechnology) in the presence of 0.1 mM EGTA and 0.5 M NaCl. Beads were then washed five times with washing buffer (50 mM Tris buffer [pH 7.4] containing 0.1 mM EGTA, 5% glycerol, 0.5 M NaCl, 0.1% β-mercaptoethanol, and protease inhibitors). For coimmunoprecipitation assays, 50 μl of anti-TgLRR1 antiserum or control serum was incubated for 4 h at 4°C with 100 μl of protein G-Sepharose in 0.5 ml of TNE (50 mM Tris, 0.1% NP-40, 2 mM EDTA). Total protein extracts or subcellular fractions were then added to the mixture. After an overnight incubation at 4°C, Sepharose beads were extensively washed in TNTE (TNE plus 0.1% Triton X-100). In all experiments, bound proteins were eluted with loading buffer (200 mM Tris, 2% SDS, 5% glycerol, 1% β-mercaptoethanol), separated by SDS-PAGE, transferred to nitrocellulose filters, and subjected to immunoblot analysis with TgLRR1 and PP1 antibodies.

Measurement of mRNA levels by RT-PCR. *T. gondii* cysts were isolated from brains of chronically infected mice. In vivo bradyzoites were freed by pepsin digestion (0.05 mg/ml pepsin in 170 mM NaCl and 60 mM HCl) for 5 to 10 min at 37°C. These in vivo bradyzoites and tachyzoites cultivated in HFF were lysed with 1% SDS, 50 mM sodium acetate (pH 5.2), and 10 mM EDTA, and total RNA was isolated following two phenol extractions at 65°C and ethanol precipitation. For controls, total RNA from uninfected brain cells of mice and HFF were also isolated. For RT-PCR, total RNA was digested with DNase and checked by PCR that no DNA remained in these samples before reverse transcription was done, as previously described (16). Semiquantitative RT-PCR was performed by using 10-fold serial dilutions of tachyzoite and bradyzoite cDNAs. The cDNA products were amplified with 50 pmol of each primer in the presence of 1 μl of Clontech *Taq* mixture DNA polymerase (Clontech) in 50-μl reaction mixture volumes. Thermal cycling conditions were denaturation at 94°C for 10 min (1); denaturation at 94°C for 45 s, followed by annealing at 60°C for 1 min and 30 s (2); elongation for 1 min and 30 seconds at 72°C (3); and at the end, an additional extension for 10 min at 72°C (4). Usually, 40 cycles were performed. Primers used in this study were as follows: 5′-ATGCCGGACGACACGAGGACAGCAGGACCCCCAGC-3′ and 5′-TCAAGCGTTGTGCTTCATAATGGACTTCTGCTTTG-3′ for TgLRR1, 5′-ATGGTGTCATTAGACGTCGATGTCGACGCC-3′ and 5′-TTATTTGGCCATGCCTTTCTTCTTTTCCAC-3′ for TgPP1, and 5′-ATGGCGGATGAAGAAGTGCAA-3′ and 5′-GATGCACTTGCGGTGGACGAT-3′ for *T. gondii* actin. PCR products were separated by electrophoresis in agarose gels, stained with ethidium bromide, scanned, and quantified using Image J software.

Immunofluorescence assays. Purified extracellular tachyzoites were fixed with 4% paraformaldehyde solution in PBS for 30 min and loaded onto slides until dry. The parasites were incubated with mouse antisera anti-PP1 or anti-TgLRR1. For double-labeling staining, parasites were sequentially incubated with mouse antiserum anti-PP1 and with rabbit antiserum anti-ROP1 (a generous gift from Jean-François Dubremetz, University of Montpellier, France). After the slides were washed, the secondary antibody goat anti-mouse labeled with Alexa Fluor 488 (green) and/or the secondary antibody goat anti-rabbit labeled with Alexa Fluor 594 (red) (Molecular Probes, The Netherlands) was used. After the slides were washed, the parasite nuclei were stained with propidium iodine for 15 min. Cover slides were mounted, and slides were examined by confocal microscopy (LSM 510; Zeiss) and by fluorescence microscopy (Leica) at a magnification of ×100, using a charge-coupled-device (CDD) camera (Leica) piloted by Metaview software.

Transient transfection of *T. gondii*. For transfection of *T. gondii*, the *T. gondii PP1* (Tg*PP1*) and Tg*LRR1* genes were generated by PCR using the following flanking primers: TgLRR1 (NsiI) forward (5′-ATGCATGACGACACGAGGACAGCAGGACCC-3′), TgLRR1 (PacI) reverse (5′-TTAATTAACTAAGCGTTGTGCTTCATAATGGACTTCTG-3′), TgPP1 (EcoRI) forward (5′-GAATTCATGCAGGAGCAGAAGCTCATCTCCGAGGAGGACCTGGCCATGGCCATGGTGTCATTAGACGTCGATGTCGACGCCG-3′), and TgPP1 (PacI) reverse (5′-TTAATTAATTATTTGGCCATGCCTTTCTTCTTTTCCACTGG-3′), respectively. The forward primer of TgPP1 contains a nucleotide sequence coding for the cMyc-Tag. PCR products were cloned in TA cloning vector and sequenced. The amplified DNA was digested with NsiI/PacI for TgLRR1 and EcoRI/PacI for TgPP1, after which the gel was purified and ligated into a *T. gondii* vector whose expression is driven by tubulin promoter (37). The constructs were used to transform *Escherichia coli* JM109 cells, and the plasmid inserts were verified by sequencing with pTUBF (5′-CGCACGAAGGGGATGTGTCAGAAAC-3′) and pTUBR (5′-GGTGGCGGCCGCTCTAGAACTAG-3′).

For *T. gondii* transient transfections, 50 μg of circular plasmids of TgLRR1-cMyc and TgPP1-cMyc were electroporated into 5.0×10^6 tachyzoites of the 76K strain and resuspended in 800 μl of cytomix buffer (120 mM KCl, 0.15 mM $CaCl_2$, 10 mM K_2HPO_4/KH_2PO_4 [pH 7.6], 25 mM HEPES [pH 7.6], 2 mM EGTA, 5 mM $MgCl_2$) containing 2 mM ATP (pH 7.5) and 5 mM glutathione. Electroporation was done in a 4-mm gap cuvette using a BTX electrocell manipulator 600 (BTX, San Diego, CA) set at a voltage of 2.5 kV · cm^{-1}, 25-μF capacitance, and 48-Ω serial resistance (37). Electroporated parasites were immediately allowed to infect slides containing confluent monolayer HFF for about 4 h. After cells were washed with fresh culture medium, transfected tachyzoites were allowed to grow for 24 h. The intracellular tachyzoites were fixed with 4% paraformaldehyde in PBS and washed three times with PBS. After the cells were permeabilized with 0.2% Triton X-100 in PBS for 30 min at room temperature, the slides were incubated with a monoclonal antibody specific to c-Myc, which was prepared in PBS containing 0.1% Triton X-100 and 10% FCS. After three washes, the slides were incubated with fluorescein isothiocyanate-coupled goat anti-mouse IgG. For parasite-stable transfection, linearized plasmids TgLRR1-cMyc and TgPP1-cMyc using KpnI were purified by phenol-chloroform extraction. Ten micrograms of linearized Tub5-Bleo-3′SAG1 plasmid for bleomycin selection was added to 90 μg of linearized TgLRR1-cMyc and TgPP1-cMyc, and transfection of tachyzoites was performed as described above. The transfected parasites were loaded onto confluent monolayer HFF and grown until cell lysis. Purified extracellular tachyzoites were incubated with 5 μg · ml^{-1} of bleomycin in DMEM-10% FCS for 8 to 10 h at 37°C. Then, they were loaded again onto HFF cells under drug pressure for 48 h. The drug selection was repeated three times, and emerging resistant parasites were processed for immunofluorescence assays.

Preparation of TgLRR1 cRNA and microinjection into *Xenopus* oocytes. Capped mRNA (cRNA) was synthesized using a T7 or SP6 mMessage mMachine kit (Ambion). TgLRR1-pCDNA3-V5 was linearized by PmeI. cRNAs transcribed from 1.5 μg of linearized plasmid were precipitated by 2.5 M LiCl, washed in 70% ethanol, resuspended in 20 μl of diethyl pyrocarbonate-treated water, and quantified by spectrophotometry. Finally, 1 μg of cRNA was analyzed with a denaturing agarose gel. Gel staining with 10 μg · ml^{-1} ethidium bromide allowed confirmation of the size of cRNA and the absence of abortive transcripts. cRNA control was obtained from the Grb2 P49L-pSP64T construct, as previously described.

Preparations of *Xenopus* oocytes and microinjection experiments were performed as previously described (41). In each assay, 20 oocytes removed from two to three different animals were microinjected with different concentrations of okadaic acid (OA), anti-PP1 antibodies, TgLRR1 cRNA, or Grb2 P49L cRNA. GVBD was detected by the appearance of a white spot at the center of the animal pole. Western blotting analysis was performed after electrophoresis. The membranes were developed with anti-PP1 serum diluted to 1:50. To detect TgLRR1, we used the anti-V5 monoclonal antibody (1:5,000). Antibody complexes were detected using an advanced chemiluminescence Western blotting detection system (Amersham).

For assessment of phosphatase activity, *Xenopus* oocytes that had undergone 100% GVBD were collected after microinjection of OA or anti-PP1 serum or TgLRR1 cRNA and lysed in PBS buffer supplemented with protease inhibitors (Sigma). Lysates were cleared by three successive centrifugations, and the total phosphatase activity was assayed using 100-μl equivalents to extracts of seven oocytes, as described above.

Nucleotide sequence accession numbers. The nucleotide sequences reported in this paper have been submitted to the GenBank Data Bank with accession numbers DQ437870 for TgLRR1 and DQ437871 for TgPP1.

RESULTS

Identification of *T. gondii* PP1. Analyses of TgPP1 by using ToxoDB, Genefinder, TigrScan, and GLmHMM predicted three potential open reading frames in a single genomic locus that differed mainly at their N termini. RT-PCR results re-

```
TgPP1  MVSLDVDVDAVISKLLEVRGSRPGKPVQLTEAEIRGLCHKSREIFISQPILLELEAPIK  59
PfPP1    MALEIDIDNVISKLIEVRGTRPGKNVNLTENEIKILCLSSREIFLNQPILLELEAPIK  58
HsPP1 MSDSEKLNLDSIIGRLLEVQGSRPGKNVQLTENEIRGLCLKSREIFLSQPILLELEAPLK  60

TgPP1 ICGDIHGQYYDLLRLFEYGGFPPEANYLFLGDYVDRGKQSLETICLLLAYKIKYPENFFL  119
PfPP1 ICGDIHGQFYDLLRLFEYGGFPPDANYLFLGDYVDRGKQSLETICLLLAYKIKYPENFFL  118
HsPP1 ICGDIHGQYYDLLRLFEYGGFPPESNYLFLGDYVDRGKQSLETICLLLAYKIKYPENFFL  120

TgPP1 LRGNHECASINRIYGFYDECKRRYNIKLWKTFTDCFNCLPVAAIIDEKIFCMHGGLSPEL  179
PfPP1 LRGNHECASINRIYGFYDECKRRYSVKLWKTFIDCFNCLPVAAIIDEKIFCMHGGLSPEL  178
HsPP1 LRGNHECASINRIYGFYDECKRRYNIKLWKTFTDCFNCLPIAAIVDEKIFCCHGGLSPDL  180

TgPP1 NSMDQIRRIVRPTDVPDIGLLCDLLWSDPEKEISGWGENDRGVSFTFGQDVVHNFLRKHD  239
PfPP1 NNMEQIRKITRPTDVPDNGLLCDLLWSDPEKEINGWGENDRGVSFTFGQDVVHNFLRKHE  238
HsPP1 QSMEQIRRIMRPTDVPDQGLLCDLLWSDPDKDVQGWGENDRGVSFTFGAEVVAKFLHKHD  240

TgPP1 LDLICRAHQVVEDGYEFFAKRQLVTLFSAPNYCGEFDNAGAMMSVDETLMCSFQILKPVE  299
PfPP1 LDLICRAHQVVEDGYEFFAKRQLVTLFSAPNYCGEFDNAGAMMSVDETLMCSFQILKPVE  298
HsPP1 LDLICRAHQVVEDGYEFFAKRQLVTLFSAPNYCGEFDNAGAMMSVDETLMCSFQILKPAD  300

TgPP1 KKKGMAK                                                       306
PfPP1 KKKAAN                                                        304
HsPP1 KNKGKYGQFSGLNPGGRPITPPRNSAKAKK                                 330
```

FIG. 1. Protein sequence alignment of TgPP1 with human and *P. falciparum* PP1s (accession nos. P62136 and AAM54063, respectively). Identical amino acid residues are shaded. The six-amino-acid sequence specific for Ser/Thr phosphatases is boxed.

vealed that the TgGeneFinder_5784 prediction (gene accession number 583.m05380) was correct. Using 5′ and 3′ RACE approaches and cDNA sequencing, we confirmed an open reading frame of 921 bp. Examination of the nucleotide sequence obtained with that of the genomic sequence showed that the gene is composed of five exons interrupted by four introns and encodes 306 amino acids. Comparative analysis of the deduced amino acid sequence showed 89% and 90% identity with human (accession number P62136) and *P. falciparum* PP1s (accession number AAM54063), respectively (Fig. 1). The amino acid sequence contains the LRGNHE signature (positions 120 to 125) of Ser/Thr phosphatases. It was noted that the human PP1 is 23 amino acids longer than TgPP1.

In order to demonstrate that the predicted TgPP1 is functionally active, recombinant TgPP1 was expressed in *E. coli* and purified as soluble and active recombinant protein. Different batches were used to normalize the phosphatase activity of TgPP1 by using a standard curve constructed with recombinant rabbit PP1 with known specific activity. This allowed us to define 5 units of TgPP1 as the value that gave 1 absorbance unit after a 1-h incubation period at 37°C in the presence of 1 mM $MnCl_2$ and 5 mM pNPP. The optimum pH of rTgPP1 was 7.4 ± 0.2. As expected, we found that okadaic acid could inhibit the activity of TgPP1 by 95% at a final concentration of 5 μM, with a 50% inhibitory concentration (IC_{50}) of about 70 nM (Fig. 2A). In addition, the effect of phosphatidic acid, a specific inhibitor of PP1 (28), on rTgPP1 activity was tested. As expected, results obtained showed clearly that rTgPP1 was sensitive to phosphatidic acid, and its phosphatase activity was reduced by about 50% in the presence of 62 nM of this compound (data not shown). Recombinant TgPP1 was characterized next with respect to its dependence on divalent cations. In the presence of $MgCl_2$, phosphatase activity was barely detectable (Fig. 2B). However, the inclusion of Mn^{2+} dramatically stimulated the phosphatase activity of TgPP1 toward pNPP,

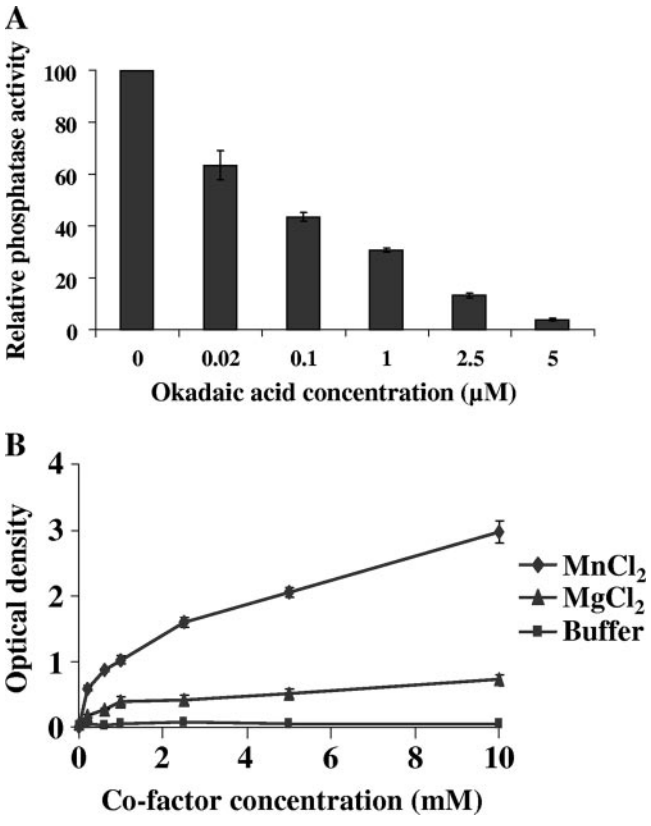

FIG. 2. Biochemical characterization of rTgPP1. (A) Effect of okadaic acid on rTgPP1 activity. pNPP (5 mM) was incubated with rTgPP1 (5 units) in the presence of different concentrations of OA (0 to 5 μM). (B) Activity of rTgPP1 in the presence or absence of divalent cations. rTgPP1 (5 units) was incubated in the presence of $MgCl_2$ or $MnCl_2$ (0 to 5 mM). Results are the means of three different experiments in triplicate with three different batches of rTgPP1.

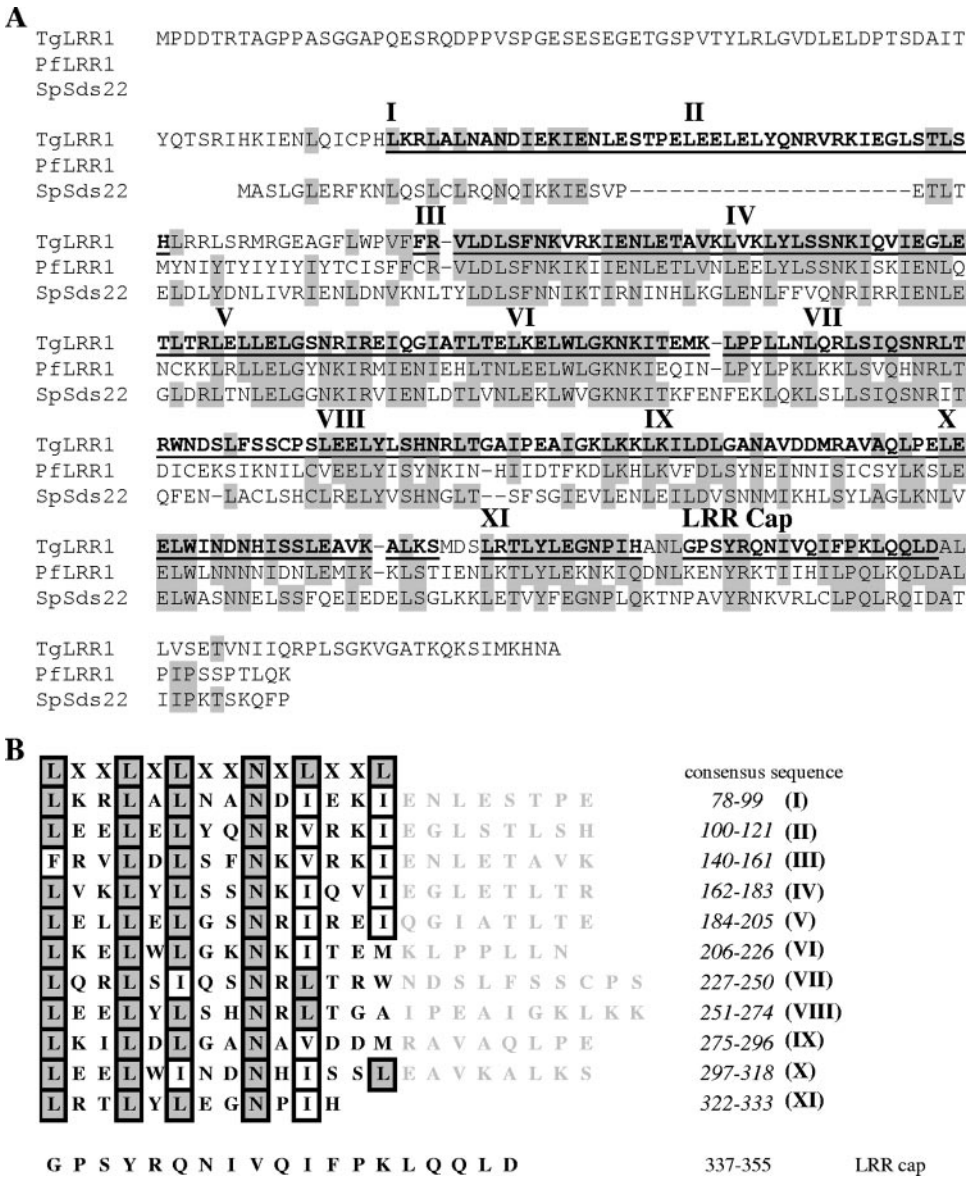

FIG. 3. (A) Protein sequence alignment of TgLRR1 with *S. pombe* Sds22 and PfLRR1 (accession nos. AAA35342 and AAX86874, respectively). Identical residues are shown in gray. The LRR motifs are in bold type and numbered from I to XI. The LRR motifs and the LRR cap sequences are underlined. (B) LRR motifs of TgLRR1. Numbers in the column at the right indicate the amino acid positions of each LRR motif. The N (position IX) and L/I (position XI) are highly conserved, and only 8 repeats out of 11 exactly fit the consensus.

with an approximate sixfold increase compared to that of $MgCl_2$. These results demonstrated that TgPP1 is similar to all known PP1s and shares the same biochemical characteristics.

Identification of TgLRR1 and sequence analysis. BLASTP analysis of the ToxoDB database (http://www.ToxoDB.org) revealed the presence of a single gene (ToxoDB identifier TgTwinScan_3263; gene accession number 57.m01867) encoding a protein with 30% identity with the fission yeast *S. pombe* protein $SpSds22^{+}$; it is well-known that this protein interacts with protein phosphatase type 1. RT-PCR showed the presence of one product whose size agreed with the predicted open reading frame. In order to determine the start and stop codon positions, 5′ and 3′ RACE approaches were used. Sequencing of PCR and RACE products revealed that the full open reading frame is present on a 1,164-bp cDNA fragment, designated TgLRR1. Comparison of the cDNA and the genomic sequence revealed that the Tg*LRR1* gene is composed of 10 exons and 9 introns.

On the basis of the nucleotide sequences that we determined, the deduced open reading frame contained a polypeptide of 388 amino acids with a calculated molecular mass of 43.5 kDa. In reciprocal BLASTP searches of the GenBank database, the highest score was obtained with its paralogue in *P. falciparum*, PfLRR1 (49% identity) (Fig. 3A). The aligned region of TgLRR1 spanned almost the complete sequence, covering residues 72 to 366, and contains 11 putative LRRs (Fig. 3B). These LRRs contain the consensus sequence LXX

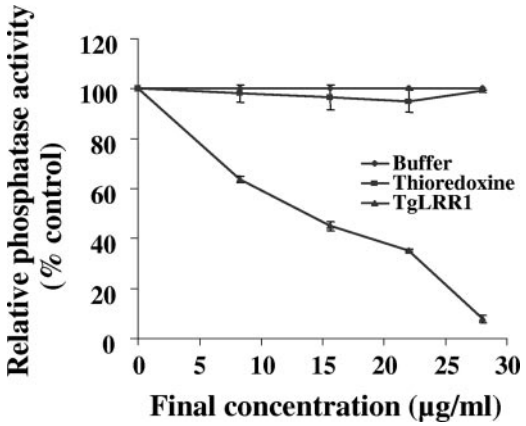

FIG. 4. Effect of TgLRR1 on TgPP1 phosphatase activity. Recombinant TgPP1 was preincubated for 1 h at room temperature with different concentrations of TgLRR1 before testing for phosphatase activity. ◆, activity in medium alone (100%); ■, relative activity in the presence of thioredoxin protein control (no inhibition was observed whatever the concentration used); ▲, relative activity in the presence of different concentrations of recombinant TgLRR1. Results of three representative experiments performed in triplicate (means ± standard deviations [error bars]) are shown.

LXLXXNXL (where X is any amino acid), where the LXX LXL motif constitutes a β strand, and XXNXL corresponds to the α turn structure. In general, the LRR motifs are involved in protein-protein interaction. The 19 carboxy-terminal residues (positions 337 to 355) of TgLRR1 constitute a conserved structure, designated LRR cap (Fig. 3B). The position of the LRR cap relative to those of the other LRRs is also indicated in Fig. 3A. It was proposed that this structure plays a role in shielding the hydrophobic core of the LRR superhelix from solvent (8). Analyses of the N-terminal portion, using the Signal P program, did not predict the presence of a signal peptide in TgLRR1.

Inhibition of TgPP1 activity by TgLRR1. In previous studies, TgLRR1 orthologs, such as SpSds22 and PfLRR1, were shown to bind PP1 but with completely different effects on its activity. Indeed, SpSds22 enhanced the activity of SpPP1; however, PfLRR1 has been shown to be a negative regulator of PfPP1. To investigate the role of TgLRR1, recombinant TgPP1 was preincubated for 1 h with different concentrations of recombinant TgLRR1 and then tested for phosphatase activity. As shown in Fig. 4, incubation of TgPP1 with TgLRR1 before testing enzymatic activity lowered phosphatase activity in a dose-dependent manner. About 90% inhibition was obtained at concentrations between 25 and 30 μg/ml of TgLRR1. The IC_{50} value obtained, based on the predicted molecular mass of TgLRR1, is 3.2 μM. Recombinant thioredoxin protein used as control did not show any significant inhibition. These results, unlike those obtained with SpSds, which promotes an activation of PP1, support the idea that TgLRR1 can be considered as an inhibitor of TgPP1.

To further confirm the inhibitory role of TgLRR1 and since PP1s are very well conserved among different species, we used the *Xenopus* oocyte model. In this model, it has been shown that the microinjection of either OA or anti-PP1 antibodies (39) can trigger meiotic progression, leading to oocyte GVBD. If TgLRR1 inhibited the PP1 activity against its natural substrates, then the expression of TgLRR1 in oocytes should lead to GVBD. We therefore microinjected TgLRR1 cRNA into oocytes and monitored the appearance of GVBD side by side with those injected with OA and anti-PP1 antibodies. Twenty-four hours postmicroinjection of TgLRR1, more than 90% of oocytes underwent GVBD, and similar results were obtained with OA or anti-PP1 antisera (Fig. 5A). Control injections of buffer, preimmune sera, or irrelevant cRNA did not trigger GVBD. The time course of GVBD appearance revealed that TgLRR1 cRNA induced GVBD with a certain delay (50% GVBD at 8 h) compared to that of OA or anti-PP1 antibodies (data not shown). This can be explained by the translational step required to produce sufficient amounts of the protein. In this context, detectable amounts of V5-tagged protein of the expected size appeared in oocyte extracts 10 h postmicroinjection (Fig. 5B). In order to explain the effect of TgLRR1 in this oocyst system, we checked whether TgLRR1 protein could bind to *Xenopus* oocyte PP1 as well. As can be seen in Fig. 5C, immunoblotting analysis of the same eluate from microcystin-agarose, an affinity column known to specifically bind PP1, revealed the presence of both *Xenopus* oocyte PP1 and TgLRR1, whereas the eluate of control oocytes that did not receive TgLRR1 cRNA revealed only the presence of PP1. In addition, the effect of TgLRR1 on the endogenous phosphatase activity of injected oocytes was also demonstrated. In these experiments, 24 h after microinjection of TgLRR1 cRNA or anti-PP1 sera, 100% of oocytes underwent GVBD, and we observed 40 to 55% inhibition of phosphatase activity compared to that of oocyte controls injected either with irrelevant cRNA or preimmune antisera or vehicle (Fig. 5D). Therefore, these results provide further support that TgLRR1 can function as a repressor of PP1 in the *Xenopus* oocyte system.

Expression of the Tg*LRR1* and Tg*PP1* genes in tachyzoite and bradyzoite stages. From the above results, it is suggested that a decrease of PP1 activity by TgLRR1 leads to the reinitiation of the cell cycle in *Xenopus*. Thus, we reasoned that TgLRR1 and/or TgPP1 may be differentially expressed between the rapidly replicating tachyzoites and the quiescent bradyzoites. To this end, total RNA purified from tachyzoites and bradyzoites was used in RT-PCR with TgLRR1- and TgPP1-specific primers. Three serial dilutions, from 1:1 and 1:10 to 1:100, of cDNA templates were tested. As shown in Fig. 6A, the transcriptional level of TgPP1 did not vary between the tachyzoite and bradyzoite stage. In contrast, the level of TgLRR1 mRNA was lower in the slowly dividing bradyzoites than in the rapidly replicating tachyzoites (Fig. 6A). In bradyzoites, only a weak TgLRR1 mRNA band could be seen at dilution 1:10, and no product was amplified at dilution 1:100, whereas a strong amplification was still evident in tachyzoites at the same dilution. As a control, the *T. gondii* actin housekeeping gene was compared (Fig. 6A). To investigate the expression at the protein level, antibodies raised against recombinant TgLRR1 were used to detect native TgLRR1 in parasite extracts. Immunoblot analysis revealed one polypeptide of an apparent molecular mass of 44 kDa that is consistent with the predicted protein sizes (Fig. 6B, lanes 1 and 2). Using anti-PP1, one polypeptide of 35 kDa, consistent with the predicted molecular mass was also detected (Fig. 6B, lanes 3 and 4). Interestingly, the protein signal of TgLRR1 was found to be stron-

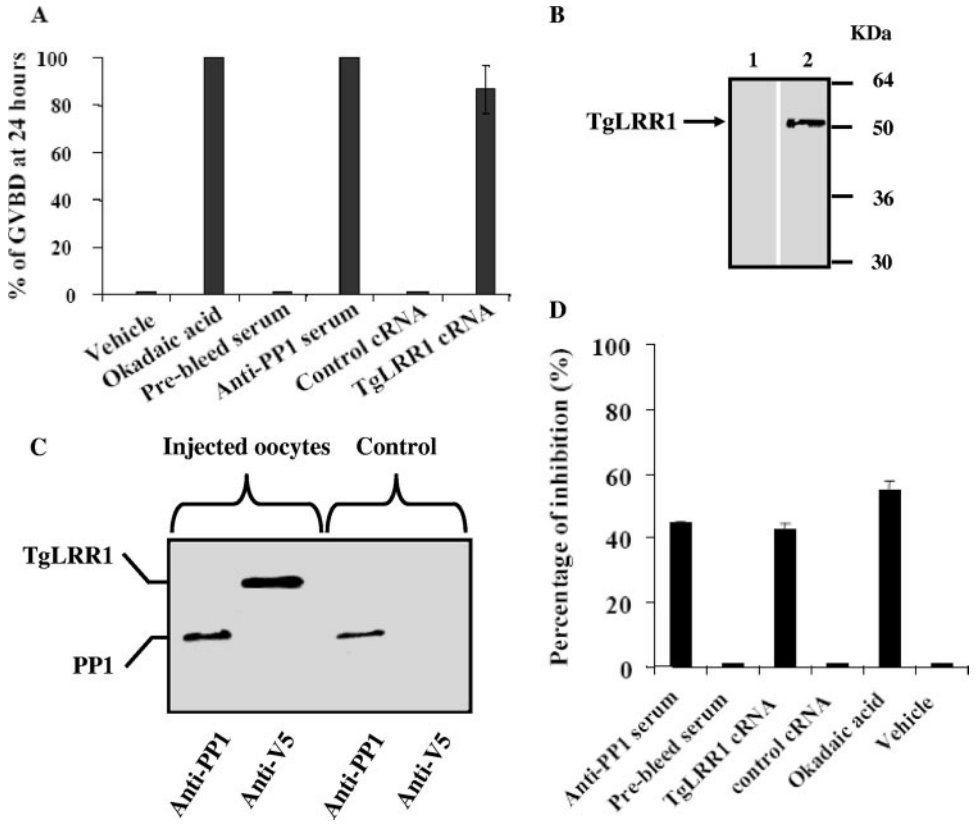

FIG. 5. Induction of GVBD in *Xenopus* oocytes. (A) Appearance of GVBD at 24 h postmicroinjection. A total volume of 100 nanoliters was used for each microinjection. Okadaic acid, anti-PP1 antisera, and TgLRR1 cRNA were used at 10 μM, 100 nl, and 150 ng, respectively. Buffer alone represents the negative control of okadaic acid (0% GVBD compared to OA, 100%). Prebled serum represents the negative control of anti-PP1 antisera (0% GVBD, compared to anti-PP1 antisera, 100%). Grb2 P49L cRNA represents the negative control of TgLRR1 cRNA (0% GVBD, compared to TgLRR1 cRNA, 94%). Results of three independent experiments are presented as the mean percentages ± standard deviations (error bars) (total number of oocytes used was 60, obtained from two to three different animals). (B) Expression of TgLRR1 protein by *Xenopus* oocytes microinjected with TgLRR1 cRNA. Immunoblot analysis was performed with oocytes injected with vehicle (lane 1) or TgLRR1 cRNA (lane 2) and revealed with anti-V5 antibodies. The arrow indicates TgLRR1. (C) Interaction of TgLRR1 with *Xenopus* oocyte PP1. Immunoblot analysis of eluates from oocyte extracts after binding to microcystin beads, as revealed either by anti-PP1 antibodies or anti-V5 antibodies. The first two lanes correspond to TgLRR1 cRNA-injected oocyte eluates, and the last two panels correspond to eluates of buffer-injected oocytes. (D) Inhibition of total phosphatase activity in oocyte extracts microinjected either with anti-PP1 serum (100 nl) or with TgLRR1 cRNA (150 ng). Phosphatase activity was measured at 24 h postmicroinjection (100% GVBD). Results are presented as the percentage of inhibition in comparison with oocytes that received either control prebled sera or control cRNA and are the means of three independent experiments. For comparison, inhibition of total phosphatase activity was performed with okadaic acid (55% inhibition was obtained at 10 μM). Phosphatase activity was assessed with microinjected oocyte extracts (100% GVBD).

ger in tachyzoites than in bradyzoites (Fig. 6B, lanes 1 and 2), consistent with the RT-PCR data (compare Fig. 6A and B). As expected, the levels of TgPP1 and actin gene products were similar in both tachyzoites and bradyzoites (Fig. 6B, lanes 5 and 6). These results indicate that the Tg*LRR1* gene is differentially expressed in tachyzoites and bradyzoites, while the Tg*PP1* gene is constitutively expressed in these two parasite stages.

Localization of TgLRR1 and TgPP1. The subcellular localization of TgLRR1 and TgPP1 in *T. gondii* was analyzed by immunofluorescence. In tachyzoites, TgLRR1 was clearly present in the nucleus (green fluorescence) of all parasites examined, colocalizing with the propidium iodine (red fluorescence) (Fig. 7A). The strong nuclear localization of TgLRR1 can be seen in the yellow merged color (Fig. 7A, right panel). However, a cytoplasmic staining was also observed. When the tachyzoites were examined for the expression of TgPP1, we observed a weak but specific staining in the nucleus (Fig. 7B). In addition, we observed that polyclonal anti-PP1 antibodies revealed a signal associated with an organelle of the parasite that colocalized with staining obtained with anti-ROP1 antibodies. When bradyzoites were examined for the expression of TgPP1 and TgLRR1, the strong nuclear signal found in tachyzoites was not evident for anti-PP1 or anti-TgLRR1. Instead, a more diffuse cytoplasmic staining was observed for both proteins in bradyzoites. One representative immunofluorescence image of the bradyzoite's fluorescence is presented (Fig. 7C, TgLRR1, and D, TgPP1).

To further assess the localization patterns of TgLRR1 and TgPP1, we performed an immunofluorescence assay (IFA) of tachyzoites transfected with cMyc fused to proteins, as described in Materials and Methods. Microscopy examination of the transfected tachyzoites revealed the presence of a strong TgLRR1-cMyc signal in the cytoplasm and a weaker but con-

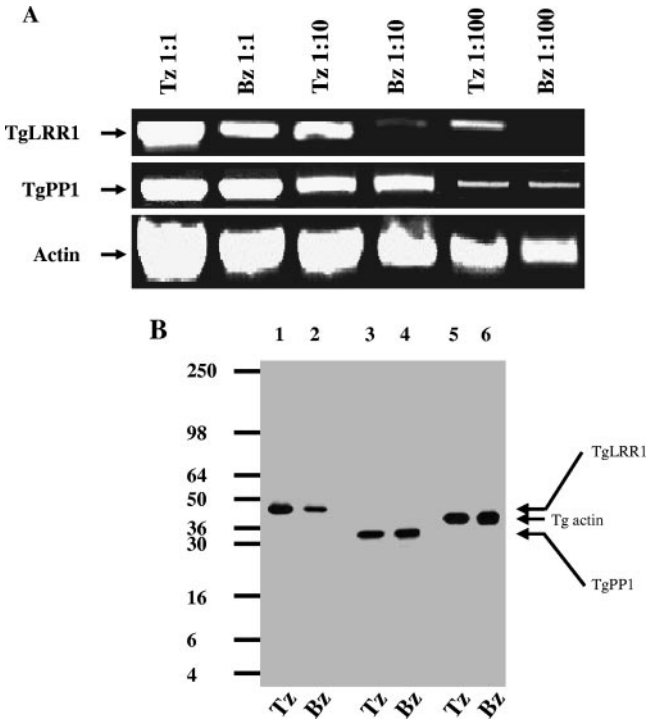

FIG. 6. (A) Expression of TgPP1 and TgLRR1 transcripts by tachyzoite and bradyzoite stages. Semiquantitative RT-PCR was performed with 10-fold serial dilutions of tachyzoite (Tz) and bradyzoite (Bz) cDNAs. To ensure that equal amounts of cDNA from each parasitic stage were being compared, actin primers were used as a control. (B) Expression of TgLRR1 and TgPP1 proteins in tachyzoite and bradyzoite stages. Western blotting analysis was performed using serum anti-TgLRR1 (lanes 1 and 2) raised against recombinant protein or serum anti-PP1 raised against PP1 (lanes 3 and 4). To ensure that equal amounts of proteins from each parasitic stage were being compared, monoclonal antibodies specific for actin were used as a control (lanes 5 and 6).

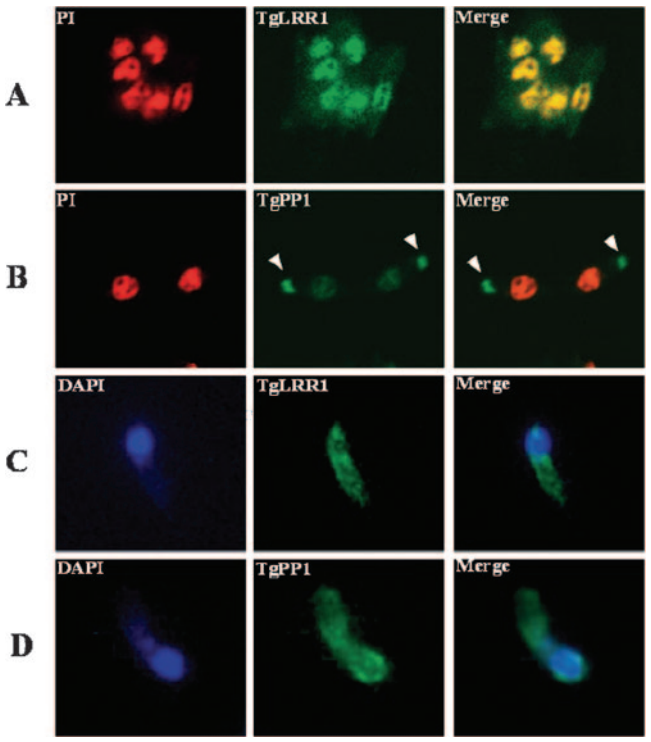

FIG. 7. Extracellular tachyzoites immunolabeled with various primary antibodies visualized with fluorescein isothiocyanate (green) or rhodamine (red). In panels A and B, the nuclei were stained with propidium iodine (PI) (red), and in panel C, they were stained with DAPI (blue). In panels A and B, immunofluorescence was obtained by confocal microscopy. (C and D) Immunofluorescence was examined with a fluorescence microscope (Leica) at a magnification of ×100, equipped with a charge-coupled-device camera (Leica) piloted by Metaview software. (A) Tachyzoites showing a nucleocytoplasmic localization for TgLRR1, with a strong nuclear labeling. The strong nuclear localization of TgLRR1 can be seen in the yellow merged color. (B) Tachyzoites showing a nucleocytoplasmic localization of TgPP1 with a substantial staining of the nucleus but a strong labeling of secretory organelles named rhoptries. (C) Immunofluorescence labeling of bradyzoite using anti-TgLRR1. (D) Immunofluorescence labeling of bradyzoite using anti-TgPP1.

sistent nuclear signal (Fig. 8, two upper sets). Transfection of the TgPP1-cMyc also showed an intense cytoplasmic fluorescence, and a part of the signal overlaps that of the nuclear 4,6-diamidino-2-phenylindole (DAPI) staining (Fig. 8, two lower sets). Using confocal fluorescence microscopy, we were unable to detect fluorescence in other subcellular compartments except for that described for the cytoplasm and the nucleus, suggesting that the rhoptry signal observed as described above corresponds to a cross-reactivity of the polyclonal antibodies to TgPP1-unrelated proteins of this organelle.

Interaction of TgLRR1 and TgPP1 in *T. gondii*. From the viewpoint of protein structure, TgLRR1 contains 11 copies of LRR motifs which form a "horseshoe" structure (data not shown; Conserved Domain Database program; http://130.14.29.110/Structure/cdd/cdd.shtml) capable of mediating an interaction with TgPP1. We have focused our investigation on the interaction that can occur between the native TgLRR1 and TgPP1 in the tachyzoites, as we failed to obtain sufficient encysted bradyzoites from mouse brain for these biochemical studies. Similar to the interaction between TgLRR1 and the heterologous PP1 of *Xenopus* oocyte shown in Fig. 5, immunoblot analysis of the tachyzoite proteins binding to microcystin beads, with anti-PP1 or anti-TgLRR1 antibodies, revealed the presence of both TgLRR1 and TgPP1 in the eluates (Fig. 9A, lanes 3 and 4). To further ascertain the interaction between TgLRR1 and TgPP1, immunoprecipitation experiments with anti-TgLRR1 antibodies were performed. Again, immunoblot analysis of proteins eluted from the anti-TgLRR1 column confirmed that PP1 had been coimmunoprecipitated with the TgLRR1 from the parasite extracts (Fig. 9B, lanes 3 and 4).

Based on the nucleocytoplasmic localization, we next examined whether the TgLRR1-TgPP1 interaction can take place in both compartments. The cytoplasmic and nuclear fractions were isolated from tachyzoites, and the components of these two subcellular fractions were checked by immunoblotting. The quality control of the subcellular fractionation was checked for the presence of the parasite cytoplasmic marker LDH1, which is detected only in the cytoplasmic fraction (Fig. 9C, compare lanes 1 and 2), whereas the nuclear marker *T. gondii* DNA repair enzyme (TgDRE) was found predominantly in the nuclear fraction (Fig. 9C, compare lanes 3 and 4).

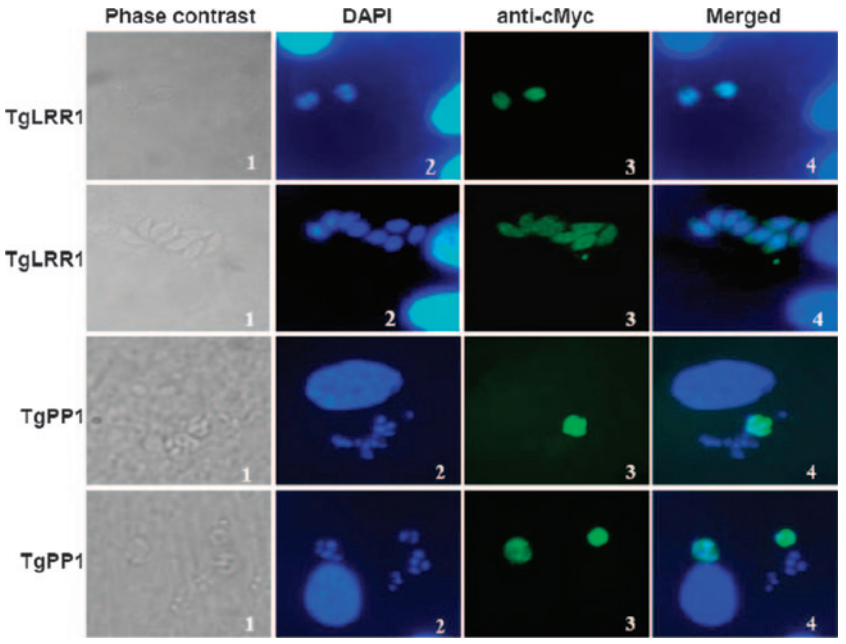

FIG. 8. Localization of *T. gondii* tachyzoites TgLRR1 and TgPP1 using transient transfection assays. Two independent sets of data for TgLRR1-cMyc are shown (two upper sets, magnification ×100). Panel 1, phase contrast; panel 2, DAPI staining; panel 3, IFA using anti-cMyc; panel 4, merged DAPI and IFA. Two independent sets of data for TgPP1-cMyc are shown (two lower sets, magnification ×65). Panel 1, phase contrast; panel 2, DAPI staining; panel 3, IFA using anti-cMyc; panel 4, merged DAPI and IFA. Note that TgLRR1 and TgPP1 signals are predominantly seen in the parasite's cytoplasm, whereas a weak but consistent nuclear fluorescence can be observed.

Immunoblotting with anti-TgLRR1 and anti-PP1 antibodies clearly confirmed that TgPP1 (Fig. 9C, lanes 5 and 6) and TgLRR1 (lanes 7 and 8) were present in the nuclear fractions and in the cytoplasmic fractions, supporting the data for immunofluorescence localization. We then investigated whether TgLRR1 and TgPP1 could interact in both cytoplasmic and nuclear fractions. Although TgLRR1 was detected in the cytoplasm, Western blotting of the proteins retained on the microcystin beads revealed the presence of TgPP1 alone (Fig. 9D, lanes 1 and 2). However, the microcystin pull down experiments using the nuclear fraction showed that TgLRR1-TgPP1 exists as a complex in this compartment (Fig. 9D, lanes 3 and 4). Similar results have been obtained with coimmunoprecipitation experiments using anti-TgLRR1 antibodies (data not shown). Taken together, these data demonstrate that the interaction between TgLRR1 and TgPP1 takes place only in the nuclear compartment of the rapidly dividing and virulent tachyzoites. The absence of this complex in the cytoplasm of tachyzoites may be due to the association of TgPP1 with other partners. This is supported by the Coomassie blue staining of the SDS-polyacrylamide gels using cytoplasm eluates which revealed the presence of several bands (data not shown).

DISCUSSION

In this work we have characterized TgPP1 and a partner belonging to the family TgLRR1 that downregulates TgPP1 activity. PP1 is a highly conserved member of the protein serine-threonine phosphatases that play important roles in a wide range of cellular functions (7). In *T. gondii*, a study combining the use of protein phosphatase inhibitors and biochemical analysis suggests that the activity of phosphatase type 1 detected in invasive tachyzoites is implicated in the control of the host cell invasion process (14). *T. gondii* genome analyses revealed the presence of three potential ORFs present on the same genomic locus. RT-PCR with primers derived from the predicted ORFs, combined with 5′ and 3′ RACE approaches, allowed the identification of one correct ORF. The two other possible ORFs failed to yield PCR products from *T. gondii* cDNA. Comparative analysis of the deduced amino acid sequence showed a high degree of identity (>85%) with several known PP1s, including human and *P. falciparum* counterparts. Furthermore, the TgPP1 sequence revealed a near-perfect alignment of the catalytic domain (positions 10 to 303) and the presence of the LRGNHE signature sequence of Ser/Thr phosphatases. To characterize and study the properties of TgPP1, we expressed and purified the corresponding recombinant protein. This was catalytically active, with an increased activity in the presence of $MnCl_2$, and was inhibited by the addition of okadaic acid in a dose-dependent manner. These observations are in agreement with previous data obtained with PP1 from different organisms (11, 12). With respect to the expression of TgPP1 by *T. gondii*, immunoblotting data showed the presence of one specific band at the expected size in both tachyzoites and bradyzoites, suggesting the absence of important post-translational modifications which could affect the protein mobility on SDS-polyacrylamide gels. Our data are consistent with previous studies that have described the expression of one PP1 isoform by tachyzoites (14).

The location of TgPP1 in the nucleus and cytoplasm of wild-type or transiently transfected tachyzoites of *T. gondii* supports the idea that its different locations may account for the diversified action of this phosphatase. PP1 has also been

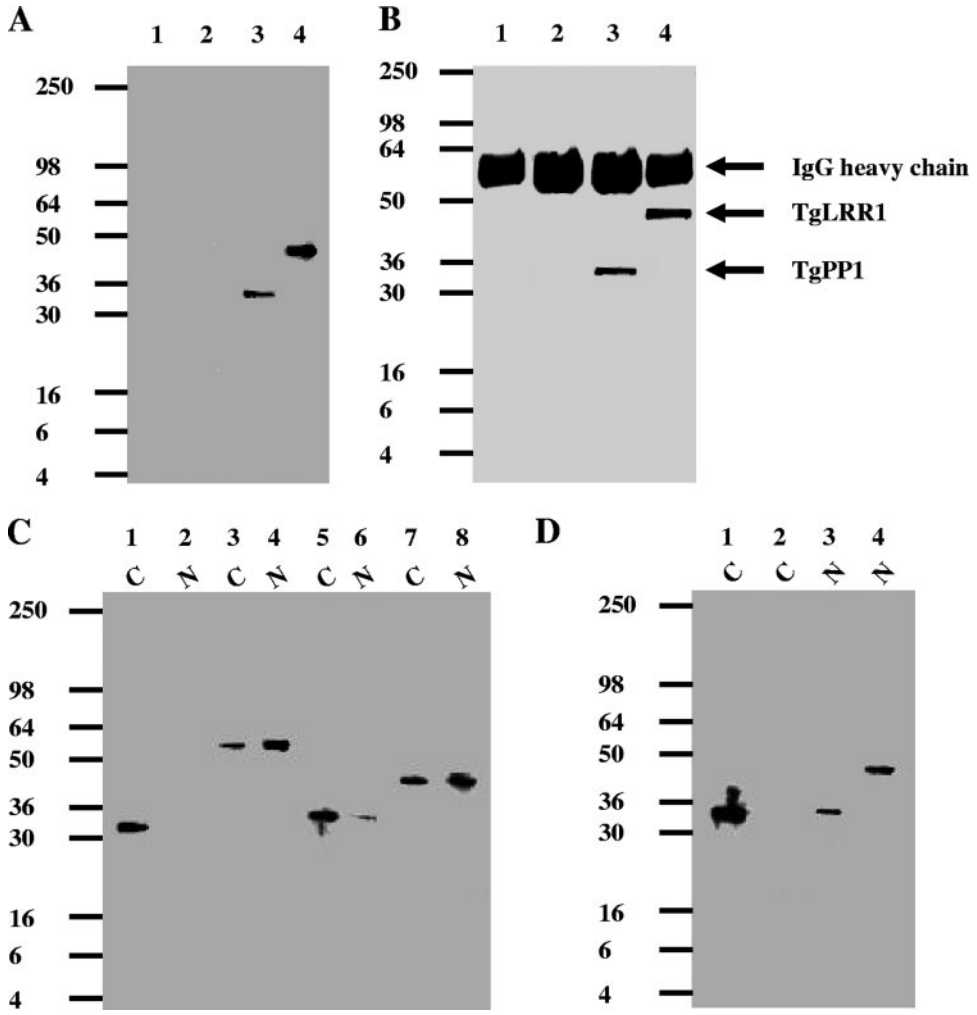

FIG. 9. Interaction of TgLRR1 with TgPP1 in *T. gondii* extracts. (A) Immunoblot analysis of proteins eluted from microcystin-agarose incubated with whole-parasite extracts. Identical quantities of the eluate were loaded onto four different lanes, separated by SDS-PAGE, and transferred to nitrocellulose. Lanes 1 and 2 are negative controls (beads incubated with buffer, without *T. gondii* protein extracts). Lanes 3 and 4 show the detection of TgPP1 and TgLRR1, which were, respectively, probed with specific polyclonal anti-PP1 and anti-TgLRR1 antibodies. (B) Coimmunoprecipitation of the TgLRR1-TgPP1 complex with anti-TgLRR1 antibodies from *T. gondii* extracts. Immunoprecipitates from control preimmune sera or from anti-TgLRR1 antisera were eluted, separated by SDS-PAGE, and transferred to nitrocellulose. Immunoblot analysis was performed with anti-PP1 (lanes 1 and 3) and anti-TgLRR1 antibodies (lanes 2 and 4). The bands at 55 kDa detected in all lanes represent the heavy chains of the antibodies bound to protein G-Sepharose. (C) Immunoblot analysis of cytoplasmic and nuclear fractions. Cytoplasmic (C) (lanes 1, 3, 5, and 7) and nuclear (N) (lanes 2, 4, 6, and 8) fractions were probed with different antibodies. Lanes 1 and 2 were probed with using anti-LDH1 antibodies, a cytoplasmic marker. Lanes 3 and 4 were probed with anti-TgDRE, a *T. gondii* DNA repair enzyme. Lanes 5 and 6 were probed with anti-PP1 antibodies. Lanes 7 and 8 were probed with anti-TgLRR1. Note that TgLRR1 and TgPP1 were detected in both cytoplasmic and nuclear fractions. (D) Immunoblot analysis of cytoplasmic (C) (lanes 1 and 2) or nuclear (N) (lanes 3 and 4) fractions eluted from microcystin-agarose. Identical quantities of the eluate were loaded onto four different lanes, separated by SDS-PAGE, and transferred to nitrocellulose. Lanes 1 and 3 were probed with anti-PP1 antibodies. Lanes 2 and 4 were probed with anti-TgLRR1 antibodies.

reported to be located in the nucleus in mammals (20). Then, how does TgPP1 localize to the nucleus? Using a Signal P-NN program for predicting subcellular localization signals (http://www.cbs.dtu.dk), TgPP1 did not show a nuclear location signal (NLS). However, using psortII (http://psort.ims.u-tokyo.ac.jp), a classical "pat7" NLS at the C-terminal side was predicted (PXXKKK) (23). Given the different locations of TgPP1, it is likely that its localization may depend upon another protein(s) for targeting to the various organelles. In quiescent bradyzoites, TgPP1 was found mainly in the cytoplasm. Even if we cannot exclude the possibility that a tiny amount of TgPP1 could also be present in the bradyzoite's nucleus, it appears that the nuclear signal of TgPP1 is stronger in tachyzoites than that found in bradyzoites. A similarly distributed nucleocytoplasmic pattern has been reported for PP1 in mammalian cells where it is located in the cytoplasm in quiescent cells, but increased amounts are detected in the nucleus upon entry of cells into the mitotic cycle (20).

Extensive knowledge has been accumulating about the importance of mammalian and yeast PP1 in metabolism, protein synthesis, control of microtubule dynamics, and cell division via the dephosphorylation process. Moreover, PP1 activities

are known to be regulated through several regulatory proteins. A variety of studies have identified more than 10 proteins in yeast and about 25 proteins in mammals that control the activity of PP1 and/or determine its specific substrate (7). One such regulatory partner is the gene protein product Sds22 that was found to play a key role in the control of mitosis in yeast (33, 38). Furthermore, it has been shown that Sds22 can directly bind to PP1 in both mammals and yeast (9, 32). In the present work, evidence for the presence of an Sds22 ortholog in *T. gondii*, TgLRR1, has been obtained. TgLRR1 is made up of a tandem array of 11 so-called LRRs of about 22 amino acids, spanning 66% of the protein. In agreement with the known function of LRR motifs as ligand-interacting modules (25), the repeat region of TgLRR1 seems very likely to participate in the interaction with TgPP1. Indeed, bioinformatics analyses predicted that it adopts a horseshoe shape, commonly observed in the Sds22 protein family. Further analysis of the C terminus revealed the presence of the LRR cap composed of 19 amino acids (positions 337 to 355) that perfectly matches the consensus sequence described by Ceulemans et al. (8). The LRR cap was proposed to play a role in the protection of the hydrophobic core formed by the LRR motifs (8). More importantly, the finding that expression of the *SDS22* gene lacking the C terminus excluded the corresponding protein from the nucleus of yeast indicates an essential nuclear targeting signal in the LRR cap region (38). Using psortII, we did not observe an NLS in this region of TgLRR1, but the overall examination of the sequence revealed a nuclear prediction of 70% (35). In *T. gondii*, immunofluorescence assays showed the presence of TgLRR1 in the cytoplasm of all bradyzoites examined; however, in tachyzoites, TgLRR1 was found in both the cytoplasmic and nuclear compartments, with intense staining in the latter area. As the TgLRR1 product was detected at the same size in both stages, its presence in the nuclei of tachyzoites and not of bradyzoites could be explained either by the expression of a specific transporter in the former and/or by the fact that TgLRR1 has to reach an expression threshold to get into the nucleus. Transient transfection of *T. gondii* with a TgLRR1 construct fused to cMyc, which allowed microscopy detection, showed staining in both the cytoplasm and nucleus. Further studies of TgPP1 or TgLRR1 in *T. gondii* have been hampered by the inability to obtain stable parasites expressing TgLRR1-cMyc or TgPP1-cMyc, suggesting that overexpression of either TgLRR1 or TgPP1 protein could be toxic to parasite growth.

To explore experimentally the predicted interaction between TgLRR1 and TgPP1, we performed coimmunoprecipitation experiments using anti-TgLRR1 antibodies and affinity chromatography on a matrix of microcystin, a cyclic heptapeptide that dramatically inhibits PP1. Both approaches revealed that TgLRR1 interacts with TgPP1 in tachyzoite extracts, in that we could show the coprecipitation of TgLRR1 and TgPP1 by immunoblotting. This association raised the question of a possible regulatory effect on TgPP1. Using recombinant TgPP1 and TgLRR1 expressed in *E. coli*, we demonstrated downregulation of the phosphatase activity. These results, unlike those observed for the Sds22 of *S. pombe*, confirmed previous observations for *P. falciparum*. The repressor function of TgLRR1 was further confirmed in a cellular context using *Xenopus* oocytes. In this model, the microinjection of TgLRR1 cRNA, like that of anti-PP1 antibodies and okadaic acid, promoted the progression of oocytes to M phase by inducing germinal vesicle breakdown. This induction paralleled an interaction of TgLRR1 with the endogenous PP1 and a decrease of about 50% in the phosphatase activity of cell extracts. This strongly suggests that downregulation of PP1 by TgLRR1 is required to initiate the cell cycle.

In light of the presence of two distinct stages in the *T. gondii* life cycle, the rapidly growing tachyzoite and the quiescent bradyzoite, together with the dynamic localization of TgLRR1 and TgPP1, we have further investigated (i) the variation in transcript levels of these genes and their products in tachyzoites versus bradyzoites and (ii) the interaction of TgLRR1 and TgPP1 in cytoplasmic and nuclear fractions of tachyzoites. Both mRNA and protein levels showed that TgPP1 was equally expressed in the two stages; however, TgLRR1 was shown to be expressed more in tachyzoites. Moreover, the TgLRR1-TgPP1 complex was detected only in the nuclear fraction, thus confirming the colocalization of both of the proteins observed in tachyzoites. The use of bradyzoites in these experiments was hampered by the quantity and quality of fractions that can be obtained.

In conclusion, although the possible link between the expression of TgLRR1 in the nuclei of tachyzoites and the capacity of these parasites to replicate rapidly, compared to bradyzoites, remains to be determined, our findings are consistent with the hypothesis that downregulation of dephosphorylation through interaction with TgLRR1 in the nuclei of tachyzoites may be a prerequisite for cell division. Conversely, lower levels of nuclear TgLRR1 may be a hallmark of slowly growing encysted bradyzoites.

ACKNOWLEDGMENTS

This work was supported by the INSERM U547-Université Lille II, Pasteur Institute of Lille, and the CNRS. Wassim Daher and Gabrielle Oria were supported by fellowships from the Fondation des Treilles and the Ministère de l'Enseignement Supérieur et de la Recherche (MESR), respectively. Wassim Daher gratefully acknowledges the current financial support of a European Molecular Biology Organization (EMBO) long-term fellowship.

We thank the Toxoplasma Genome Sequencing Consortium for making available the genome database at http://ToxoDB.org.

REFERENCES

1. **Al-Anouti, F., S. Tomavo, S. Parmley, and S. Ananvoranich.** 2004. The expression of lactate dehydrogenase is important for the cell cycle of *Toxoplasma gondii*. J. Biol. Chem. **279:**52300–52311.
2. **Black, M. W., and J. C. Boothroyd.** 2000. Lytic cycle of *Toxoplasma gondii*. Microbiol. Mol. Biol. Rev. **64:**607–623.
3. **Bollen, M., and W. Stalmans.** 1992. The structure, role, and regulation of type 1 protein phosphatases. Crit. Rev. Biochem. Mol. Biol. **27:**227–281.
4. **Bradley, P. J., and J. C. Boothroyd.** 2001. The pro region of Toxoplasma ROP1 is a rhoptry-targeting signal. Int. J. Parasitol. **31:**1177–1186.
5. **Bradley, P. J., C. Ward, S. J. Cheng, D. L. Alexander, S. Coller, G. H. Coombs, J. D. Dunn, D. J. Ferguson, S. J. Sanderson, J. M. Wastling, and J. C. Boothroyd.** 2005. Proteomic analysis of rhoptry organelles reveals many novel constituents for host-parasite interactions in *Toxoplasma gondii*. J. Biol. Chem. **280:**34245–34258.
6. **Carter, A. O., and J. W. Frank.** 1986. Congenital toxoplasmosis: epidemiologic features and control. Can. Med. Assoc. J. **135:**618–623.
7. **Ceulemans, H., and M. Bollen.** 2004. Functional diversity of protein phosphatase-1, a cellular economizer and reset button. Physiol. Rev. **84:**1–39.
8. **Ceulemans, H., M. De Maeyer, W. Stalmans, and M. Bollen.** 1999. A capping domain for LRR protein interaction modules. FEBS Lett. **456:**349–351.
9. **Ceulemans, H., A. Van Eynde, E. Perez-Callejon, M. Beullens, W. Stalmans, and M. Bollen.** 1999. Structure and splice products of the human gene encoding sds22, a putative mitotic regulator of protein phosphatase-1. Eur. J. Biochem. **262:**36–42.
10. **Coppin, A., F. Dzierszinski, S. Legrand, M. Mortuaire, D. Ferguson, and S.**

Tomavo. 2003. Developmentally regulated biosynthesis of carbohydrate and storage polysaccharide during differentiation and tissue cyst formation in *Toxoplasma gondii*. Biochimie **85:**353–361.

11. **Daher, W., E. Browaeys, C. Pierrot, H. Jouin, D. Dive, E. Meurice, C. Dissous, M. Capron, S. Tomavo, C. Doerig, K. Cailliau, and J. Khalife.** 2006. Regulation of protein phosphatase type 1 and cell cycle progression by PfLRR1, a novel leucine-rich repeat protein of the human malaria parasite *Plasmodium falciparum*. Mol. Microbiol. **60:**578–590.
12. **Daher, W., K. Cailliau, K. Takeda, C. Pierrot, N. Khayath, C. Dissous, M. Capron, M. Yanagida, E. Browaeys, and J. Khalife.** 2006. Characterization of *Schistosoma mansoni* Sds homologue, a leucine-rich repeat protein that interacts with protein phosphatase type 1 and interrupts a G2/M cell-cycle checkpoint. Biochem. J. **395:**433–441.
13. **Delorme, V., X. Cayla, G. Faure, A. Garcia, and I. Tardieux.** 2003. Actin dynamics is controlled by a casein kinase II and phosphatase 2C interplay on *Toxoplasma gondii* toxofilin. Mol. Biol. Cell **14:**1900–1912.
14. **Delorme, V., A. Garcia, X. Cayla, and I. Tardieux.** 2002. A role for *Toxoplasma gondii* type 1 ser/thr protein phosphatase in host cell invasion. Microbes Infect. **4:**271–278.
15. **Dendouga, N., I. Callebaut, and S. Tomavo.** 2002. A novel DNA repair enzyme containing RNA recognition, G-patch and specific splicing factor 45-like motifs in the protozoan parasite *Toxoplasma gondii*. Eur. J. Biochem. **269:**3393–3401.
16. **Dzierszinski, F., M. Mortuaire, N. Dendouga, O. Popescu, and S. Tomavo.** 2001. Differential expression of two plant-like enolases with distinct enzymatic and antigenic properties during stage conversion of the protozoan parasite *Toxoplasma gondii*. J. Mol. Biol. **309:**1017–1027.
17. **Dzierszinski, F., O. Popescu, C. Toursel, C. Slomianny, B. Yahiaoui, and S. Tomavo.** 1999. The protozoan parasite *Toxoplasma gondii* expresses two functional plant-like glycolytic enzymes. Implications for evolutionary origin of apicomplexans. J. Biol. Chem. **274:**24888–24895.
18. **Eaton, M. S., L. M. Weiss, and K. Kim.** 2006. Cyclic nucleotide kinases and tachyzoite-bradyzoite transition in *Toxoplasma gondii*. Int. J. Parasitol. **36:** 107–114.
19. **Ferguson, D. J., S. F. Parmley, and S. Tomavo.** 2002. Evidence for nuclear localisation of two stage-specific isoenzymes of enolase in *Toxoplasma gondii* correlates with active parasite replication. Int. J. Parasitol. **32:**1399–1410.
20. **Fernandez, A., D. L. Brautigan, and N. J. Lamb.** 1992. Protein phosphatase type 1 in mammalian cell mitosis: chromosomal localization and involvement in mitotic exit. J. Cell Biol. **116:**1421–1430.
21. **Gilbert, L. A., S. Ravindran, J. M. Turetzky, J. C. Boothroyd, and P. J. Bradley.** 2007. *Toxoplasma gondii* targets a protein phosphatase 2C to the nuclei of infected host cells. Eukaryot. Cell **6:**73–83.
22. **Gross, U., M. C. Kempf, F. Seeber, C. G. Luder, R. Lugert, and W. Bohne.** 1997. Reactivation of chronic toxoplasmosis: is there a link to strain-specific differences in the parasite? Behring Inst. Mitt. **99:**97–106.
23. **Hicks, G. R., and N. V. Raikhel.** 1995. Protein import into the nucleus: an integrated view. Annu. Rev. Cell Dev. Biol. **11:**155–188.
24. **Jan, G., V. Delorme, V. David, C. Revenu, A. Rebollo, X. Cayla, and I. C. Tardieux.** 2007. The toxofilin-actin-PP2c complex of *Toxoplasma*: identification of interacting domains. Biochem. J. **401:**711–719.
25. **Kedzierski, L., J. Montgomery, J. Curtis, and E. Handman.** 2004. Leucine-rich repeats in host-pathogen interactions. Arch. Immunol. Ther. Exp. (Warsaw) **52:**104–112.
26. **Kibe, M. K., A. Coppin, N. Dendouga, G. Oria, E. Meurice, M. Mortuaire, E. Madec, and S. Tomavo.** 2005. Transcriptional regulation of two stage-specifically expressed genes in the protozoan parasite *Toxoplasma gondii*. Nucleic Acids Res. **33:**1722–1736.
27. **Kim, S. K., and J. C. Boothroyd.** 2005. Stage-specific expression of surface antigens by *Toxoplasma gondii* as a mechanism to facilitate parasite persistence. J. Immunol. **174:**8038–8048.
28. **Kishikawa, K., C. E. Chalfant, D. K. Perry, A. Bielawska, and Y. A. Hannun.** 1999. Phosphatidic acid is a potent and selective inhibitor of protein phosphatase 1 and an inhibitor of ceramide-mediated responses. J. Biol. Chem. **274:**21335–21341.
29. **Kumar, R., B. Adams, A. Oldenburg, A. Musiyenko, and S. Barik.** 2002. Characterisation and expression of a PP1 serine/threonine protein phosphatase (PfPP1) from the malaria parasite, Plasmodium falciparum: demonstration of its essential role using RNA interference. Malaria J. **1:**5.
30. **Luft, B. J., and J. S. Remington.** 1992. Toxoplasmic encephalitis in AIDS. Clin. Infect. Dis. **15:**211–222.
31. **Lyons, R. E., R. McLeod, and C. W. Roberts.** 2002. *Toxoplasma gondii* tachyzoite-bradyzoite interconversion. Trends Parasitol. **18:**198–201.
32. **MacKelvie, S. H., P. D. Andrews, and M. J. Stark.** 1995. The *Saccharomyces cerevisiae* gene *SDS22* encodes a potential regulator of the mitotic function of yeast type 1 protein phosphatase. Mol. Cell. Biol. **15:**3777–3785.
33. **Ohkura, H., and M. Yanagida.** 1991. *S. pombe* gene sds22+ essential for a midmitotic transition encodes a leucine-rich repeat protein that positively modulates protein phosphatase-1. Cell **64:**149–157.
34. **Radke, J. R., B. Striepen, M. N. Guerini, M. E. Jerome, D. S. Roos, and M. W. White.** 2001. Defining the cell cycle for the tachyzoite stage of *Toxoplasma gondii*. Mol. Biochem. Parasitol. **115:**165–175.
35. **Reinhardt, A., and T. Hubbard.** 1998. Using neural networks for prediction of the subcellular location of proteins. Nucleic Acids Res. **26:**2230–2236.
36. **Robert-Gangneux, F., C. Creuzet, J. Dupouy-Camet, and M. P. Roisin.** 2001. Mitogen activated protein kinases (MAPK) and *Toxoplasma gondii* host cell invasion. Ann. Pharm. Fr. **59:**297–304. (In French.)
37. **Soldati, D., and J. C. Boothroyd.** 1993. Transient transfection and expression in the obligate intracellular parasite *Toxoplasma gondii*. Science **260:**349–352.
38. **Stone, E. M., H. Yamano, N. Kinoshita, and M. Yanagida.** 1993. Mitotic regulation of protein phosphatases by the fission yeast sds22 protein. Curr. Biol. **3:**13–26.
39. **Swain, J. E., X. Wang, T. L. Saunders, R. Dunn, and G. D. Smith.** 2003. Specific inhibition of mouse oocyte nuclear protein phosphatase-1 stimulates germinal vesicle breakdown. Mol. Reprod. Dev. **65:**96–103.
40. **Tomavo, S.** 2001. The differential expression of multiple isoenzyme forms during stage conversion of *Toxoplasma gondii*: an adaptive developmental strategy. Int. J. Parasitol. **31:**1023–1031.
41. **Vicogne, J., K. Cailliau, D. Tulasne, E. Browaeys, Y. T. Yan, V. Fafeur, J. P. Vilain, D. Legrand, J. Trolet, and C. Dissous.** 2004. Conservation of epidermal growth factor receptor function in the human parasitic helminth *Schistosoma mansoni*. J. Biol. Chem. **279:**37407–37414.